Hydrophobe VII *7th International Conference on*
Water Repellent Treatment and Protective Surface Technology for Building Materials
A.Elena Charola and J. Delgado Rodrigues, Editors
LNEC (Laboratório Nacional de Engenharia Civil), Lisbon: 2014 (189-198)

Producing superhydrophobic coatings for roof tiles

Luis A.M. Carrascosa
Group TEP-243, Departamento de Química-Física, Facultad de Ciencias (Universidad de Cádiz), Puerto Real (Cadiz), Spain, luis.martinezcarrascosa@alum.uca.es

Dario S. Facio
Group TEP-243, Departamento de Química-Física, Facultad de Ciencias (Universidad de Cádiz), Puerto Real (Cadiz), Spain, dario.facio@uca.es

Maria J. Mosquera
Group TEP-243, Departamento de Química-Física, Facultad de Ciencias (Universidad de Cádiz), Puerto Real (Cadiz), Spain, mariajesus.mosquera@uca.es

SUMMARY: At the Universidad de Cadiz a simple and low-cost synthesis route to produce hydrophobic and water repellent coatings for building materials was developed. Specifically, the novel product has been synthesized by mixing: (1) silicon oligomers with organic radicals to reduce energy surface; (2) silica nanoparticles to create a uniform roughness surface, providing water repellent properties; (3) n-octylamine to prevent gel cracking and to serve as a catalyst. This sol and a commercial hydrophobic product (BS290) were applied on ceramic roof tile samples. The results obtained confirm the superhydrophobic behaviour of the UCA product and a longer durability than that obtained for BS290.

KEY-WORDS: superhydrophobic surfaces, nanocomposite, roof tiles, close-packed coating

INTRODUCTION

Superhydrophobicity has attracted considerable attention by their claims as water repellent and self-cleaning properties. It relies on a combination of high hydrophobicity, with contact angles over 150º, and significant water repellence, with hysteresis contact angles below 10º [1]. This last requirement is important because the contact angle hysteresis (the difference between the receding and the advancing contact angles) controls water droplet movement (i.e., the water repellent effect). Since the contact angle on smooth hydrophobic surfaces does not exceed 120º, it is assumed that superhydrophobic surfaces can be achieved by combining two strategies: reducing the surface free energy and roughening the surface. Numerous superhydrophobic surfaces have been produced by means of a variety of techniques including etching and lithography, self-assembly and sol-gel processing, generally followed by further chemical modification. The drawback of these procedures is that they involve tedious and multi-stage processes, which prevent their large-scale application, particularly on exposed surfaces of buildings and structures.

Our research group recently designed several products for restoring and protecting building materials, such as consolidant products [2], hydrophobic materials [3], and photoactive products with self-cleaning properties [4, 5]. Our products are produced by a low-cost process and, of particularly relevance, they meet the operational and commercial requirements for application to exterior surfaces of large buildings and structures. The process is so simple that the coatings are applied to the exposed surfaces requiring treatment, under outdoor conditions, using common methods such as brushing or spraying.

Recently, we have developed a low-cost one-step synthesis to produce superhydrophobic coatings for exposed surfaces of buildings and other structures [6]. Specifically, we have mixed silica nanoparticles with a silica oligomer and a low molecular weight organic siloxane in presence of a surfactant. The organic component reduces the surface energy, thus giving a valuable hydrophobic property and the nanoparticles create a water-repelling surface roughness. There are two fundamental reasons for adding a surfactant (such as *n*-octylamine) to our sol: (1) to produce a gel network with a coarse the pore structure, preventing cracking [7]; and, (2) to act as a basic catalyst of the sol-transition on the substrate surface [2]. Finally, it is significant that volatile organic compounds (VOCs) are not added to the sol. The volatile organic solvents were avoided for two reasons: to produce "green" products; and to enhance the products dry matter depostion in order to increase their effectiveness [2].

In this paper, the previously synthesized product was applied on commonly used ceramic roof tiles and its effectiveness was evaluated. For comparison, a commercial hydrophobic product was evaluated. Finally, an in-depth investigation of the surface roughness of the treated tiles was carried out in order to establish relationships between hydrophobic behavior and surface morphology.

EXPERIMENTAL SECTION

Synthesis

According to a previous work developed in our researcher group [6] , silica nanocomposite were prepared by mixing TES 40WN (obtained from Wacker—hereafter TES40), a hydroxyl-terminated polydimethylsiloxane (obtained from ABCR—hereafter PDMS), and AEROSIL OX50 colloidal silica particles, obtained from Evonik (hereafter OX50), in the presence of *n*-octylamine as surfactant (obtained from Aldrich). According to its technical data sheet, TES40 is a mixture of monomeric and oligomeric ethoxysilanes, with an average chain length of approximately 5 Si-O units. PDMS has a polymerization degree of 12 with a molecular mass between 400 and 700, and an OH percentage ranging from 4 to 6% w/w. OX50 is hydrophilic fumed silica with a particle diameter of 40 nm.

The starting sol was prepared according the following procedure (see Fig.1)

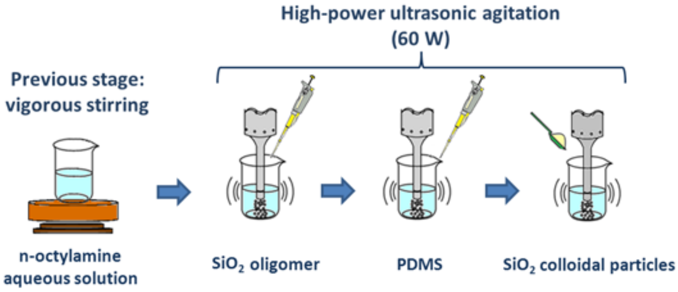

Figure 1. Synthesis route.

(1) A 1.57 M *n*-octylamine solution in water was prepared, being the concentration of the surfactant significantly higher than its critical micellar concentration (cmc), which is 0.010 M [8]. N-octylamine must be carefully manipulated because it may irritate skin, eyes and mucous membranes on contact.

(2) TES40, OX50 and the aqueous solution of *n*-octylamine were mixed under ultrasonic stirring (60 $W \cdot m^{-3}$).

(3) PDMS was further added dropwise to the mixture. The percentage of the reactants was: 89.40 %v/v TES40, 0.15 %v/v surfactant solution, and 10.45 %v/v PDMS. OX50 silica particles were added at 5 %w/v respect to the total volume of the sol. The resulting sol product was named UCA (after University of Cadiz).

This product was compared with a hydrophobic commercial product Silres BS290 from Wacker (hereafter BS290), which is a mixture of silanes and siloxanes. Following the specification of the manufacturer, it was diluted in isopropanol (hereafter ISP) at 7 %w/w.

Effectiveness on Tiles

The two products under study were applied onto ceramic roof tile samples. They were applied by three procedures: (1) spraying with an air gun with a pressure of $2 \cdot 10^5$ Pa; (2) immersion of the sample into the products for 2 min; (3) immersion during 5 min.

The samples were weighed before and after application to calculate the uptake of the products. One month later, the samples were re-weighed to calculate the products' dry matter. The characterization of the untreated tiles and their treated counterparts was carried out 1 month after application according the techniques described in the following paragraphs.

FTIR spectra of the tile samples were recorded in order to determinate the interactions produced between the products and the substrate. Spectra were obtained by using a FTIR-8400S from Shimadzu (4 cm^{-1} in resolution) in the region from 4000 to 650 cm^{-1}.

The hydrophobic behaviour was determined by the water contact angle test (sessile drop method), using a commercial video-based, software-controlled contact angle analyser, model OCA 15plus, from Dataphysiscs Instruments. Static and dynamic (advancing a receding) contact angle values were determined according to the procedure previously reported [9].

The roof tiles samples were subjected to a test of water absorption by capillarity (WAC) using a method based in UNE-EN 1925 [10].

The topography of the samples was investigated using atomic force microscopy (AM-AFM, Nanotec Electrónica S.L.) operated in tapping mode. The root-mean square (RMS) roughness values were calculated from 2.5 µm x 2.5 µm images.

Changes in colour induced by the application on samples are important. For this reason, total colour difference (ΔE^*) between untreaed and treated samples was determined using a solid reflection spectrophotometer, Colorflex model, from Hunterlab. The conditions used were: illuminant C and observer CIE 10°. $L^*a^*b^*$ scale was used, and variations in colour were evaluated.

Finally, penetration depth of the products was measured using cross-section images of the samples with a Nicon model SMZ800 stereoscopic microscope, according the following procedure: first, the samples were immersed in water; next, they were cut and visualized by microscopy. The unwetted area can be associated with the penetration depth of the products through the pore structure of the tile samples.

Durability on Tiles

In order to evaluate the durability of the treated tiles under extreme conditions, the roof tiles were subjected to an ageing test by UV light, using a Solarbox model 3000e from Cofomegra Srl. The samples were continuously illuminated with 550 W/m^2, at 50 °C, with a 80% relative humidity, for 1000 hours.

RESULTS AND DISCUSSION

Effectiveness on Tiles

After application of the products, their uptake and residual weights were measured and the average values calculated. The uptake values did not show significant differences for the products applied. However, a significant difference was observed for the different application methods, the highest corresponding to the 5 min-immersion and the lowest values for spraying, as can be seen it Table 1.

On the other hand, dry matter values obtained for the commercial product (BS290) were significantly lower than those obtained for UCA product, due to the previous dilution of BS290 in VOC. UCA product showed residue values similar to those corresponding to the uptake values because it does not contain VOCs in its composition.

Table 1. Product uptake and residual weight for the products applied on tiles, where: S: Spraying, 2’ I: 2 minutes immersion, 5’ I: 5 minutes immersion

Product	Appl.	Uptake (%)	Dry matter (%)
BS290	S	0.97 ± 0.02	0.20 ± 0.03
	2’ I	2.56 ± 0.08	0.20 ± 0.00
	5’ I	6.18 ± 0.11	0.30 ± 0.05
UCA	S	1.56 ± 0.15	1.04 ± 0.10
	2’ I	3.91 ± 0.26	2.66 ± 0.18
	5’ I	4.56 ± 0.38	2.84 ± 0.13

Table 2. Colour changes measured on the tile samples, where: S: Spraying, 2’ I: 2 minutes immersion, 5’ I: 5 minutes immersion

Product	Appl.	ΔL*	Δa*	Δb*	ΔE*
BS290	S	-5.84 ± 0.15	2.72 ± 0.02	2.72 ± 0.14	7.00 ± 0.06
	2’ I	-6.21 ± 0.22	3.12 ± 0.01	4.23 ± 0.15	8.14 ± 0.09
	5’ I	-6.93 ± 0.43	3.34 ± 0.40	3.93 ± 0.45	8.64 ± 0.71
UCA	S	-5.09 ± 0.07	1.03 ± 0.1	-0.74 ± 0.24	5.24 ± 0.12
	2’ I	-3.55 ± 0.37	-0.65 ± 0.26	-5.37 ± 0.50	6.47 ± 0.64
	5’ I	-2.91 ± 1.58	-2.71 ± 0.16	-9.06 ± 0.58	9.96 ± 0.11

The results obtained in the colorimetric study can be seen in Table 2. Both products produce a slight darkening (negative values for ΔL*) resulting in total colour variations (ΔE*) higher than the human perception threshold eye [11] (ΔE*>3) for all the samples in the study. Nonetheless, these changes were not significant for the overall appearance. The UCA product induced lower changes when sprayed or after 1 minute immersion than those corresponding to the commercial product.

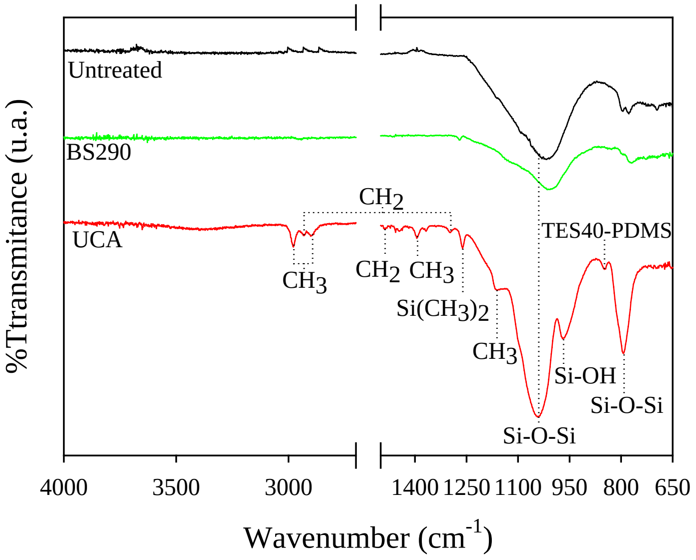

Figure 2. FTIR spectra of untreated roof tile and their treated counterparts.

FTIR spectra of the treated and untreated roof tiles (Fig. 2) emphasize the permanence of the products on the tile samples. The untreated sample showed the typical siloxane bonds from its silicate structure. It is important to emphasize that the spectra of the untreated sample was very similar to that corresponding to those treated with the commercial product confirming the low residue values obtained for the commercial product. On the other hand, samples treated with the UCA product showed new bands corresponding to alkyl groups in the range from 4000 to 1250 cm^{-1} and the methyl group band at 1260 cm^{-1} from the PDMS. In the range from 1250 to 650 cm^{-1}, the bands corresponding to siloxane bonds are present, and their intensity is higher for samples treated with UCA product (silica gel) confirming the higher residue present. Finally, it is important to mention the band around 850 cm^{-1} for the samples treated with UCA products that confirms the co-polymerization process between organic and inorganic oligomers [6, 12, 13]

Table 3 shows the static and dynamic (advancing and receding) contact angle values for the treated roof tiles and their untreated counterparts. Firstly, it must be noted that the untreated tiles show a hydrophilic behaviour, with CA values lower than 90°. For this reason their dynamic CA cannot be measured since the water droplets were absorbed. All the samples treated with the UCA product showed the highest static CA and the lowest hysteresis values. These results show that our product provides a high hydrophobicity and water repellent properties to the tile samples under study. Moreover, these values were maintained one month after application. On the other hand, the samples treated with commercial product showed suitable CA and hysteresis values immediately after application of the product. However, one month later the treated tiles lost their hydrophobic and water repellent properties, excepting for samples where the product was applied by 5 min immersion. The poor durability of BS290 can be explained by the low residue of the product left behind.

Table 3. Static contact angle (CA) values and their corresponding advancing and receding CA for untreated and treated tiles, and total water uptake (TWU); where: n.a. (not applicable as the droplets were absorbed by the tile); S: Spraying, 2'; I: 2 minutes immersion; 5' I: 5 minutes immersion.

Product	Appl.	Static CA (deg)	Advancing CA (deg)	Receding CA (deg)	Hysteresis (deg)	TWU (%)
Untreated		57 ± 1	n.a.	n.a.	n.a.	11.8
BS290	S	71 ± 1	n.a.	n.a.	n.a.	0.14
	2' I	72 ± 1	n.a.	n.a.	n.a.	0.11
	5' I	98 ± 1	n.a.	n.a.	n.a.	0.12
UCA	S	140 ± 4	138 ± 5	126 ± 4	12 ± 4	0.18
	2' I	144 ± 2	142 ± 2	133 ± 2	9 ± 4	0.23
	5' I	140 ± 2	142 ± 1	135 ± 2	7 ± 3	0.26

In order to confirm the hydrophobic behaviour of the treated tile samples, WAC test was carried out. The results obtained confirmed that water did not penetrate into the treated samples, being the total water uptake values (TWU) below 0.3% (see Table 3).

The results discussed in the previous paragraphs demonstrated that the UCA product provides superhydrophobic properties to the tile samples and is the consequence of a combination of roughness and reduction of the surface energy [14-16], Therefore the morphology of the coatings was studied in order to confirm the role played by the nanocomposite coating to produce roughness. Figure 3 shows 3D AFM images (left) and the size distribution (right) of the roughness for the roof tiles surfaces under study. Moreover, droplet pictures obtained for each surface were also included.

The morphology of the surfaces obtained permitted explaining their hydrophobic behaviour. Specifically, the untreated tile surface showed a random roughness, associated to the tile surface heterogeneity. The morphology of the tile treated with the commercial product was practically unmodified, which suggested that BS290 is not capable of covering the underlying substrate. In case of the tile treated with UCA, the morphology is significantly different. A homogeneous coating composed of densely packed uniform particles was clearly observed and can be explained as a consequence of the aggregation between the silica nanoparticles included in the starting sol and the silica particles created during sol-gel transition. Thus, larger aggregates of particles were created, as previously discussed [6]. We believe that the formation of this close-packed coating is the key factor inducing superhydrophobic behaviour, which matches with the Cassie-Baxter theory for nonwettable surfaces [14].

The roughness values obtained (see Fig. 3) showed that the average roughness value was reduced after the application of the commercial product, suggesting that this coating filled the grooves present in the untreated tile samples, while the UCA product caused an increase in the average roughness values due to the deposition the nanoparticles as described.

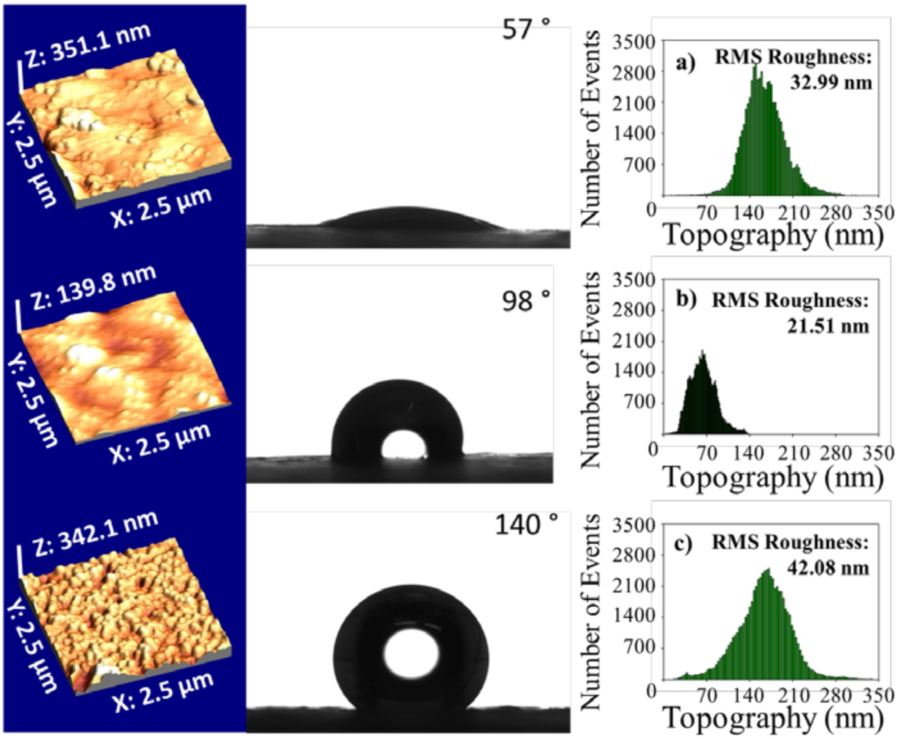

Figure 3. AFM 3D topography images and size distribution of the roughness for the surface of the untreated tile and its treated counterparts: (a) untreated, (b) BS290, (c) UCA.

Figure 4 shows the AFM 2D profiles for the surfaces under study. According to literature, the space between the textural peaks of the roughness is important for the trapping of air pockets [15, 16]. The obtained profiles present the greatest distance between peaks for untreated surfaces and those surfaces treated with BS290. In the case of the surfaces treated with UCA a lower distance between roughness peaks than that from the two other surfaces under study was clearly observed. These results match perfectly the values obtained for CA. The UCA product is able to reduce the contact area between droplet and surface, resulting in a high static CA and low adhesion. For the untreated surface and its counterpart treated with BS290, the greater spaces obtained between the roughness peaks promotes collection of water in the grooves, promoting a decrease in static CA and a higher adhesion between the water droplet and the surface. Finally, we want to remark that a reduction in roughness is observed for the surface treated with BS290. It highlights that the product partially fills the grooves of the tile, evening out the surface.

Figure 5 shows the cross-sections of the tiles under study, where the dry zones reflect the products penetration depth. The results obtained highlight that the application method is critical for the penetration depth obtained. In all the cases, the spraying procedure produced the lowest penetration depth values whereas the highest values were obtained for the 5-min immersion. Comparing the products, UCA showed the best results for the three application methods under study, particularly for spraying and 2-minute immersion.

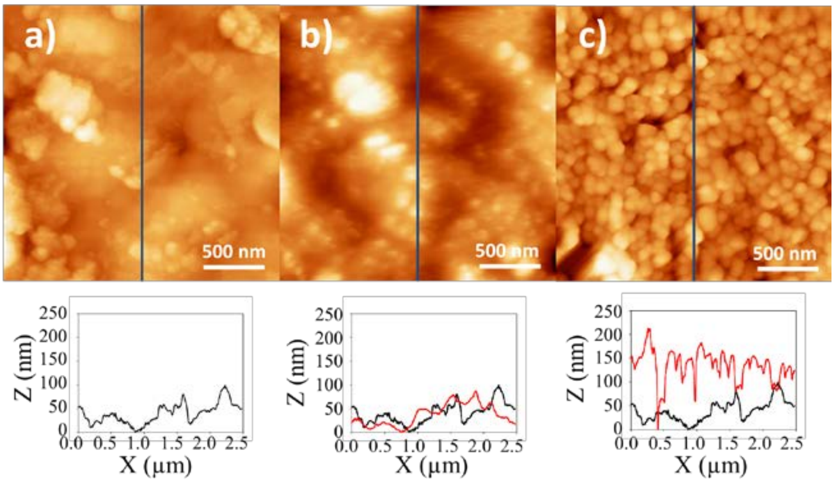

Figure 4. Roughness 2D profiles of the surface of the untreated roof tile and its treated counterparts. Blue lines show the path followed to obtain the profile: (a) untreated, (b) BS290, (c) UCA. Red line represents the roughness profile of the treated tile whereas the black line refers to the untreated one.

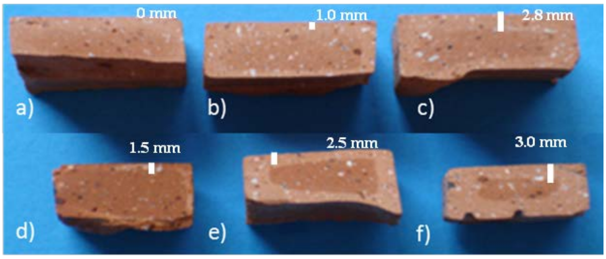

Figure 5. Cross-sections of tiles where the penetration of the product. Treated with BS290 (top): (a) Spraying, (b) 2 minutes immersion, (c) 5 minutes immersion, and treated with UCA (bottom): (d) Spraying, (e) 2 minutes immersion, (f) 5 minutes immersion.

Treatment durability

The samples under study were subjected to a durability study in climatic chamber. Two key properties were evaluated after the test: (1) colour variation; (2) contact angle values. For the former, the ageing did not modify significantly their ΔE*, which in all cases was reduced (see Table 4). For the latter (see Table 5), the samples treated with the commercial product experimented a significant reduction in their contact angle values (around 50% for spraying and 2-min immersion and 40% for 5-min immersion). Dynamic contact angles could not be measured because the samples turned hydrophilic after ageing. These results demonstrated the low durability of the commercial product, especially for roof tiles.

On the other hand, the samples treated with the UCA product had a reduction of 20% in their contact angle values (similar behaviour for static and dynamic angles). This durability can be explained due to the higher penetration depth of this product (see Fig. 5). Indeed, FTIR spectra showed a higher presence of UCA product than that from BS290 product.

Table 4. Colour change before and after ageing, where: S: Spraying, 2’ I: 2 minutes immersion, 5’ I: 5 minutes immersion

Product	Appl.	ΔE^* (before)	ΔE^* (after)
BS290	S	7.00 ± 0.06	6.47 ± 0.33
	2’ I	8.14 ± 0.09	6.18 ± 0.50
	5’ I	8.64 ± 0.71	6.69 ± 0.25
UCA	S	5.24 ± 0.12	5.18 ± 2.40
	2’ I	6.47 ± 0.64	6.19 ± 2.50
	5’ I	9.96 ± 0.11	8.10 ± 2.43

Table 5. Static and dynamic CA values for treated roof tiles after ageing, where: n.a. (not applicable as the droplets were absorbed by the tile); S: Spraying, 2’; I: 2 minutes immersion; 5’ I: 5 minutes immersion.

Product	Appl.	Static CA (deg)	Advancing CA (deg)	Receding CA (deg)	Hysteresis (deg)
Untreated		56 ± 1	n.a.	n.a.	n.a.
BS290	S	37 ± 2	n.a	n.a.	n.a.
	2’ I	39 ± 1	n.a	n.a.	n.a.
	5’ I	62 ± 5	n.a	n.a.	n.a.
UCA	S	111 ± 7	109 ± 11	96 ± 10	13 ± 3
	2’ I	112 ± 16	112 ± 7	91 ± 8	21 ± 2
	5’ I	110 ± 1	112 ± 13	94 ± 11	18 ± 1

CONCLUSIONS

From the results obtained it has been shown that a superhydrophobic coating with high durability has been produced on ceramic roof tiles by a simple and low-cost process. The novel product presents a similar cost than that corresponding to the commercial product evaluated.

From our investigation, we conclude that the addition of silica nanoparticles is a key factor in imparting the superhydrophobic property to the material. These nanoparticles produce a densely packed coating in which the air is trapped. In addition, the organic component (PDMS) reduces the surface free energy. This results in a high static contact angle and low hysteresis values.

Finally, the high durability of our product was confirmed by an accelerated ageing test. This high durability is associated to the high penetration and adherence of the product to the substrate in contrast to the commercial product evaluated, which showed poor durability.

REFERENCES

[1] GAO, L., T. McCarthy. 2006. *"Artificial Lotus Leaf" Prepared Using a 1945 Patent and a Commercial Textile*. Langmuir, 22:5998-6000.

[2] ILLESCAS, J., M. J. Mosquera. 2012. *Producing Surfactant-Synthesized Nanomaterials In Situ on a Building Substrate, without Volatile Organic Compounds*. Applied and Material Interfaces, 4:4259-4269.

[3] ILLESCAS, J., M, J. Mosquera. 2011. *Surfactant-Synthesized PDMS/Silica Nanomaterials Improve Robustness and Stain Resistance of Carbonate Stone*. Journal of Physical Chemistry **C**, 115:14624-14634.

[4] PINHO, L., M. J. Mosquera. 2011. *Titania-Silica Nanocomposite Photocatalysts with Application in Stone Self-Cleaning*. Journal of Physical Chemistry C, 115:22851-22862.

[5] PINHO, L., M. J. Mosquera. 2013. *Photocatalytic activity of TiO2-SiO2 nanocomposites applied to buildings: Influence of particle size and loading*. Applied Catalysis **B**: Environmental, 134-135:205-221.

[6] FACIO, D., M. J. Mosquera. 2013. *Simple Strategy for Producing Superhydrophobic Nanocomposite Coatings In Situ on a Building Substrate*. Applied and Material Interfaces, 5:7517-7526.

[7] MOSQUERA, M. J., D. M. de los Santos, A. Montes, L. Valdez-Castro. 2008. *New Nanomaterials for Consolidanting Stone*. Langmuir, 24:2772-2778.

[8] MIRGORODSKAYA, A., L. Kudryavtseva, Y. Zuev, V. Archipov, Z. Idiyatullin. 1999. *Catalysis of the hydrolysis of phosphorus acids esters by the mixed micelles of long-chain amines and cetylpyridinium bromide*. Mendeleev Communications, 5:196-198.

[9] MOSQUERA, M. J., D. M. de los Santos, T. Rivas. 2010. *Surfactant-Synthesized Ormosils with Application to Stone Restoration*. Langmuir, 26:6737-6745.

[10] UNE-EN 1925:1999. *Conservación del patrimonio monumental. Ensayo de ascenso capilar*.

[11] BERNS, R. 2000. *Billmeyer and Saltzman’s Principles of Color Technology*. 3rd edition. Wiley-Interscience, New York.

[12] TELLEZ, L., J. Rubio, F. Rubio, E. Morales, J. Otero. 2003. *Synthesis inorganic-organic hybrid materials from TEOS, TBT and PDMS*. Journal of Material Science, 38:1773-1780.

[13] KAPRIDAKI, C., P. Maravelaki-Kalaitzaki. 2013. TiO_2-SiO_2-*PDMS Nano-composite hydro-phobic coating with self-cleaning properties for marble protection*. Progress in Organic Coatings, 76:400-410.

[14] XU, L., R. Karunakaran, J. Guo, S, Yang. 2012. *Transparent, Superhydrophobic Surfaces from One-Step Spin Coating of Hydrophobic Nanoparticles*. Applied Materials and Interfaces, 4:1118-1125.

[15] ÖNER, D., T. McCarthy. 2000. *Ultrahydrophobic Surfaces. Effects of Topography Length Scales on Wettability*. Langmuir, 16:7777-7782.

[16] BHUSHAN, B., E. Her. 2010. *Fabrication of Superhydrophobic Surfaces with High and Low Adhesion Inspired from Rose Petal*. Langmuir, 26:8207-8217.